THE JOURNAL OF PHYSICAL CHEMISTRY A

Article

pubs.acs.org/JPCA

A Quasiclassical Study of the F(^{2}P) + CHD_3 (ν_1 = 0,1) Reactive System on an Accurate Potential Energy Surface

Juliana Palma*,† and Uwe Manthe*,‡

†Departamento de Ciencia y Tecnología, Universidad Nacional de Quilmes, Sáenz Peña 352, Bernal B1876BXD, Argentina

‡Theoretische Chemie, Fakultät für Chemie, Universität Bielefeld, Universitätsstr. 25, D-33615 Bielefeld, Germany

ABSTRACT: Quasiclassical trajectories (QCT) have been employed to elucidate the effect of exciting the C−H bond in F + CHD_3 collisions. The calculations were performed on a new potential energy surface that accurately describes the van der Waals complexes in the entrance channel of the reaction. It was found that exciting the C−H bond significantly enhances the yield of HF + CD_3, whereas it has a minor effect on the production of DF + CHD_2. Therefore, the net effect is that the total reactivity increases upon excitation. This result strongly contradicts recent experimental findings. Significant differences in regard to the yield of each product channel were also found between QCT results calculated with the new surface and those obtained with the surface previously developed by Czakó et al. This shows that relatively small variations in the topography of the entrance channel can result in huge discrepancies in the predicted DF/HF branching ratio. However, in regard to other attributes of the reaction, the agreement between QCT results computed with different surfaces, and between them and experimental results, is good. For the F + CHD_3 → HF + CD_3 reaction, at a collisional energy of 9.0 kcal/mol, experiments and QCT calculations agree, indicating that the extra energy deposited in the C−H bond is channelled into the HF product. In addition, the angular distribution of CD_3 is backward oriented and is not sensitive to the excitation of the C−H bond.

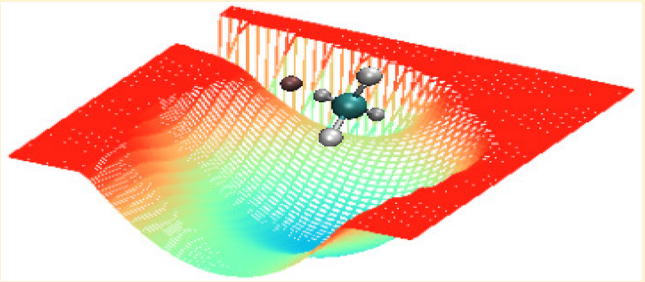

INTRODUCTION

The accurate calculation of reaction attributes for systems involving polyatomic reactants and products is a very challenging task. The existing difficulties can be readily envisaged by noting the large number of experiments on such systems that are still lacking interpretations based on accurate computations. A typical example is the investigation of the reaction between fluorine atoms and different isotopologues of methane. The last 15 years have witnessed the realization of detailed experiments on such systems, which uncovered several interesting dynamical features.[1−18] However, among those experimental results, only the photodetachment spectra of FCH_4^- and FCD_4^- (refs 17 and 18) could be contrasted against rigorous first-principle-based computations.[19−21] In other cases, quasiclassical trajectories (QCT)[22−32] or reduced dimensionality calculations[33−35] were employed to reproduce and interpret the experiments.

One of the most intriguing experimental findings about these systems is that, for the F + CHD_3 reaction, the excitation of the C−H stretching diminishes the reactivity. This result was initially reported in 2009 by Zhang et. al, who analyzed the reaction at low collisional energies (<4.0 kcal/mol).[11] More recently, Yang et al. performed a quantitative assessment on the deleterious effect of the C−H stretching excitation.[16] For the F + CHD_3 → HF + CD_3 channel at a collisional energy of 9.0 kcal/mol, they established that one quantum of excitation in the C−H stretching reduces the reactivity by ≈26%. In addition, they found that the extra energy deposited in the C−H bond is almost exclusively channelled into the HF molecule. Thus, HF molecules formed from the excited reactant are about one quantum of vibrational energy hotter than those coming from the ground-state reactant. On the contrary, the vibrational energy deposited in CD_3 is almost the same in both cases. The scattering angle distributions for CD_3 in the ground and excited-state reactions were also determined. It was found that both are backward oriented and pretty similar to each other.[16]

Quasiclassical computations by Czakó et al. found a significant suppression in the reactivity of the C−H bond with regard to the C−D bond for collisional energies <2.0 kcal/mol.[22,23] The authors explained this finding by noting that, at low energies, the excitation of the C−H bond steers the F atom toward the C−D bond. These QCT calculations were performed on a potential energy surface (PES) developed by Czakó, Shepler, Braams, and Bowman,[36] who used permutational invariant polynomials to fit 19384 UCCSD(T)/aug-cc-pVTZ-quality ab initio points. This PES did not consider the effect of the spin orbit (SO) coupling which is relevant at the entrance channel.[36] Therefore, the authors later developed a

Special Issue: Dynamics of Molecular Collisions XXV: Fifty Years of Chemical Reaction Dynamics

Received: June 28, 2015
Revised: August 11, 2015

DOI: 10.1021/acs.jpca.5b06184
J. Phys. Chem. A XXXX, XXX, XXX−XXX

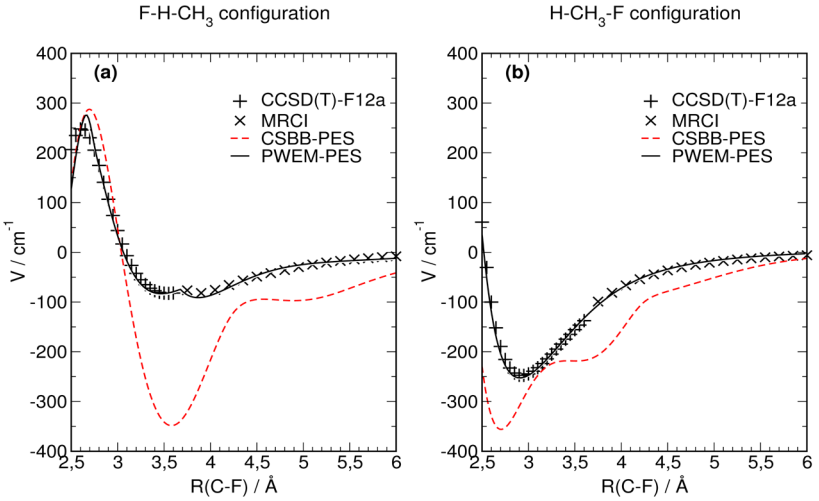

Figure 1. Ab initio and fitted surfaces without SO coupling at the entrance channel of the F + CH_4 → HF + CH_3 reaction for C_{3v} symmetry geometries. Panels a and b display results for F−H−CH_3 and H−CH_3−F configurations, respectively. The coordinates of the CH_4 molecule were frozen at their asymptotic equilibrium values. Energies are measured relative to the energy of the reactants at equilibrium in the asymptotic region.

three-dimensional SO correction.[37] When QCT computations were run on the SO-corrected surface, it was found that the surprising effect of the C−H excitation on reactivity was ameliorated. However, at 1.0 kcal/mol where the reported steering effect is the largest, the DF/HF branching ratio was still larger for the C−H excited reaction than for the ground-state reaction.[37]

Recently Westerman, Eisfeld, and Manthe presented a theoretical procedure to obtain vibronically and spin−orbit coupled diabatic PESs for the entrance channel of X + CH_4 → HX + CH_3 reactions.[20] The procedure was employed to obtain the three lowest coupled diabatic PESs of the F(^{2}P) + CH_4 → HF + CH_3 system.[20,21] The characteristics of the adiabatic surfaces derived from them were thoroughly discussed. In particular, it was demonstrated that the new adiabatic surfaces accurately describe the shape of the different van der Waals wells present in the entrance channel. In addition, full-dimensional quantum dynamical computations performed on these surfaces were able to explain the fine structure observed in the photodetachment spectra of FCH_4^- and FCD_4^-. The good agreement between theory and experiment found in this case lends further confidence on the accuracy the PESs obtained by Westerman et al.

In this article we present the results of QCT calculations aimed at analyzing the effect of the C−H excitation on F + CHD_3 collisions. Calculations were run on three alternative potential energy surfaces that differ in the topologies of their entrance channel. The results obtained with the alternative surfaces are thoroughly compared, and differences in the computed observables are discussed. A detailed comparison against the experimental findings of Zhang et al. and Yang et al. is also given.

The remainder of the article is organized as follows. The characteristics of the potential energy surfaces employed in this work are discussed in Potential Energy Surfaces, while the numerical details of the QCT computations are given in Computational Details. QCT results are presented and discussed in Results and Discussion. The comparison against experimental data is also given in Results and Discussion. Conclusions summarizes the main findings.

POTENTIAL ENERGY SURFACES

The coupled diabatic potentials of refs 20 and 21 provide an accurate description of the entrance channel of the F + CH_4 → HF + CH_3 reaction. To take advantage of it we developed a PES which combines the lowest adiabatic PES obtained from that diabatic model with the global PES developed by Czakó, Shepler, Braams, and Bowman (CSBB-PES).[36]

In refs 20 and 21, the diabatic potential energy matrix $\underline{\underline{V}}^{(\mathrm{diab})}$ describing the entrance channel of the F + CH_4 system is written as

$$\underline{\underline{V}}^{(\mathrm{diab})}(R, \theta, \phi, \mathbf{q}) = V_{\mathrm{CH_4}}(\mathbf{q})\cdot\underline{\underline{1}} + \underline{\underline{V}}^{(\mathrm{inter})}(R, \theta, \phi, \mathbf{q}) + \underline{\underline{V}}^{(\mathrm{so})} \quad (1)$$

Here $\mathbf{q}$ denotes the internal coordinates of the methane and R, θ, and ϕ are the polar coordinates associated with the vector from the carbon atom to the fluorine atom in the body fixed frame. V_{CH_4} is an adiabatic PES of the isolated methane, $\underline{\underline{V}}^{(\mathrm{inter})}$ a diabatic potential matrix describing the interaction of the F(^{2}P) atom with the CH_4 molecule, and $\underline{\underline{V}}^{(\mathrm{so})}$ a matrix describing the spin−orbit coupling in the F(^{2}P) atom. Two different parameter sets were developed by Westermann et al. for the interaction potential $\underline{\underline{V}}^{(\mathrm{inter})}$. One of them is optimized for the excited electronic state,[20] and the other one for the ground electronic state.[21] In addition, including or excluding the matrix $\underline{\underline{V}}^{(\mathrm{so})}$ in the above equation allows one to obtain potential models which either consider or otherwise neglect the spin−orbit coupling. Because of the specific ansatz used for the potential matrix, this diabatic model can not describe the breakup of the methane molecule and can be used only in the entrance channel up to the transition state.

In the present work we employed the lowest eigenvalue of matrix $\underline{\underline{V}}^{(\mathrm{diab})}$ to build a global adiabatic PES for the F + CH_4 → HF + CH_3 reaction. Consequently, the parametrization of ref 21, which guarantees an optimal description of the entrance channel in the ground-state surface, was used. This PES will be denoted V_{entr}. Two variants of V_{entr} were used: one including the spin−orbit coupling, $V_{entr\text{-}SO}$, and the other one excluding the spin−orbit coupling, $V_{entr\text{-}noSO}$. To obtain the global surface, V_{entr} was combined with the CSBB-PES. The resulting PES,

DOI: 10.1021/acs.jpca.5b06184
J. Phys. Chem. A XXXX, XXX, XXX−XXX

hereafter called PWEM-PES, switches between V_{entr} and V_{CSBB} in the transition-state region. The switching is governed by the value of the smallest of the four H−F distances, r. V_{entr} is employed if r is greater than r_{up} = 1.7 Å, while V_{CSBB} is used if r is smaller than r_{low} = 1.5 Å. Between these two domains, V_{PWEM} smoothly switches between the two PESs

$$V_{PWEM} = (1 - S(r))\cdot V_{CSBB} + S(r)\cdot V_{entr} \quad (2)$$

The switching function, $S(r)$, is given by

$$S(r) = 10.0y(r)^3 - 15.0y(r)^4 + 6.0y(r)^5$$
$$y(r) = \frac{r - r_{low}}{r_{up} - r_{low}} \quad (3)$$

Again, there are two variants of V_{PWEM}: $V_{PWEM\text{-}SO}$ is based on $V_{entr\text{-}SO}$ and includes spin−orbit coupling, while $V_{PWEM\text{-}noSO}$ is based on $V_{entr\text{-}noSO}$ and does not include spin−orbit coupling. It should be noted that spin−orbit coupling is relevant only in the entrance channel and does not affect the shape of the surfaces in the transition-state region and the product channel.

To charactize the different surfaces employed in the present work, plots of the PWEM-SO-PES, the PWEM-noSO-PES, and the CSBB-PES are shown in Figures 1 and 2. In Figure 1, the accuracy of the PESs is analyzed by comparing the fitted surfaces against results of accurate explicitly correlated coupled cluster (CCSD(T)-F12) and multireference configuration interaction (MRCI) calculations taken from refs 21 and 20, respectively. Because the ab initio calculations did not consider spin−orbit coupling, only the two PESs not including spin−orbit coupling, the PWEM-noSO-PES and the CSBB-PES, are considered. One finds that the PWEM-noSO-PES accurately reproduces the ab initio results, while significant differences between the CSBB-PES and ab initio data are observed. As already noted by Czakó et al.,[36] fitting a globally accurate F + CH_4 → HF + CH_3 PES is challenging because the energy differences in the entrance channel are very small compared to the exothermicity of the reaction. The separate construction of the entrance channel PES employed here avoids this difficulty.

The overall shape of the surfaces is presented in Figure 2. Here contour plots of the CSBB-PES, the PWEM-noSO-PES, and the PWEM-SO-PES as a function of the C−H and H−F distances are displayed. The differences between the surfaces at the entrance channel of the reaction are readily appreciated, with the CSBB-PES showing a well that is noticeably deeper and wider than that of the other two surfaces. The PWEM-SO-PES, on the other hand, is the smoothest and presents a slightly higher barrier (as expected).

We finally note that the times required to run trajectories on the PWEM-PESs and the CSBB-PES are quite different. In general, the PWEM surfaces are between 5 and 6 times slower than the CSBB-PES. For example, at a collisional energy of 9.0 kcal/mol, a batch of 2500 trajectories takes roughly 32 CPU hours on the PWEM surfaces (running on a single core of an 8 core Intel Xeon X5482 or X5550 CPU), while it takes just 6 hours on the CSBB-PES. We note that these figures just provide an average time.

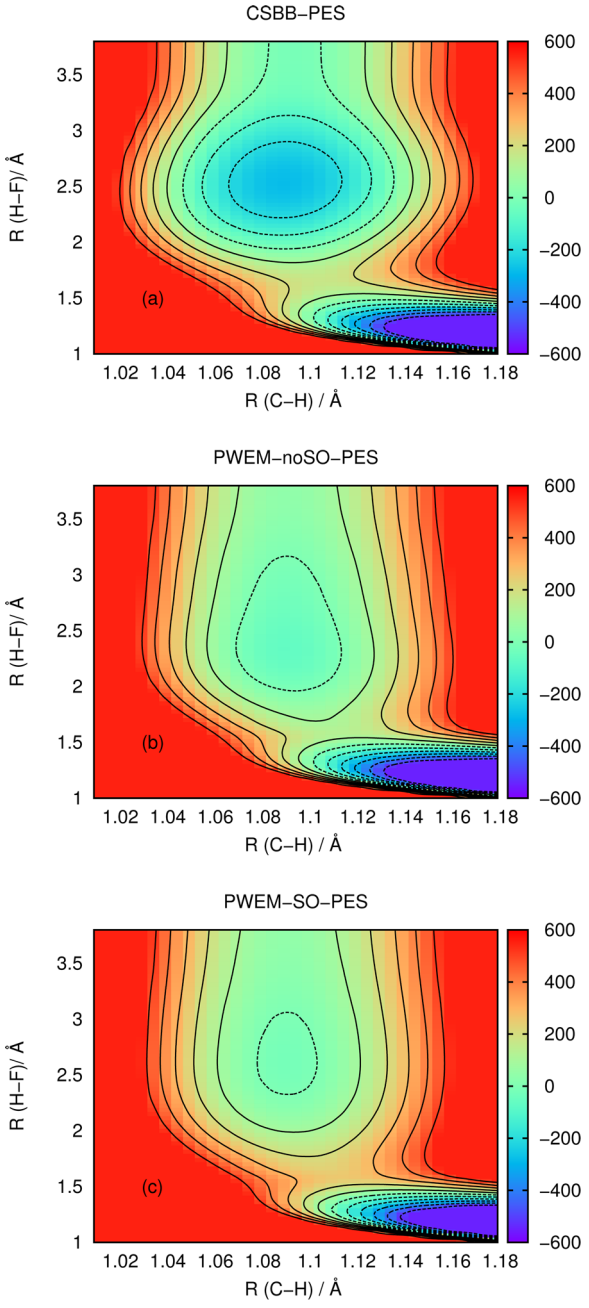

Figure 2. Contour plots as a function of the C−H and H−F distances for the F−H−CH_3 configuration. Other bonds and angles are fixed at their transition-state values. Energies are measured relative to the energy of the reactants at equilibrium in the asymptotic region. The color scheme considers only energies between −600 and 600 cm^{-1}. Contours are spaced by 100 cm^{-1} with the outermost contour set at 500 cm^{-1}. Solid lines are used for positive energies, while dashed lines are used for zero and negatives energies. The different panels display different PESs: (a) CSBB-PES, (b) PWEM-noSO, and (c) PWEM-SO.

COMPUTATIONAL DETAILS

The QCT trajectories were launched from an initial separation of 20.0a_0 between the carbon atom and the fluorine atom. The impact parameter was chosen at random from a uniform distribution between 0 and 8.0a_0. Therefore, trajectories were weighted according to the value of the selected impact parameter.[38] The initial orientation of CHD_3 was defined by randomly choosing the Euler angles that determine the orientation of its inertia axis. Standard normal mode sampling was employed to initialize the vibrational state of CHD_3, either to the ground state or to the ν_1 = 1 excited state. The standard iterative velocity adjustment was employed to set the initial angular momentum of CHD_3 to zero.[38]

DOI: 10.1021/acs.jpca.5b06184
J. Phys. Chem. A XXXX, XXX, XXX−XXX

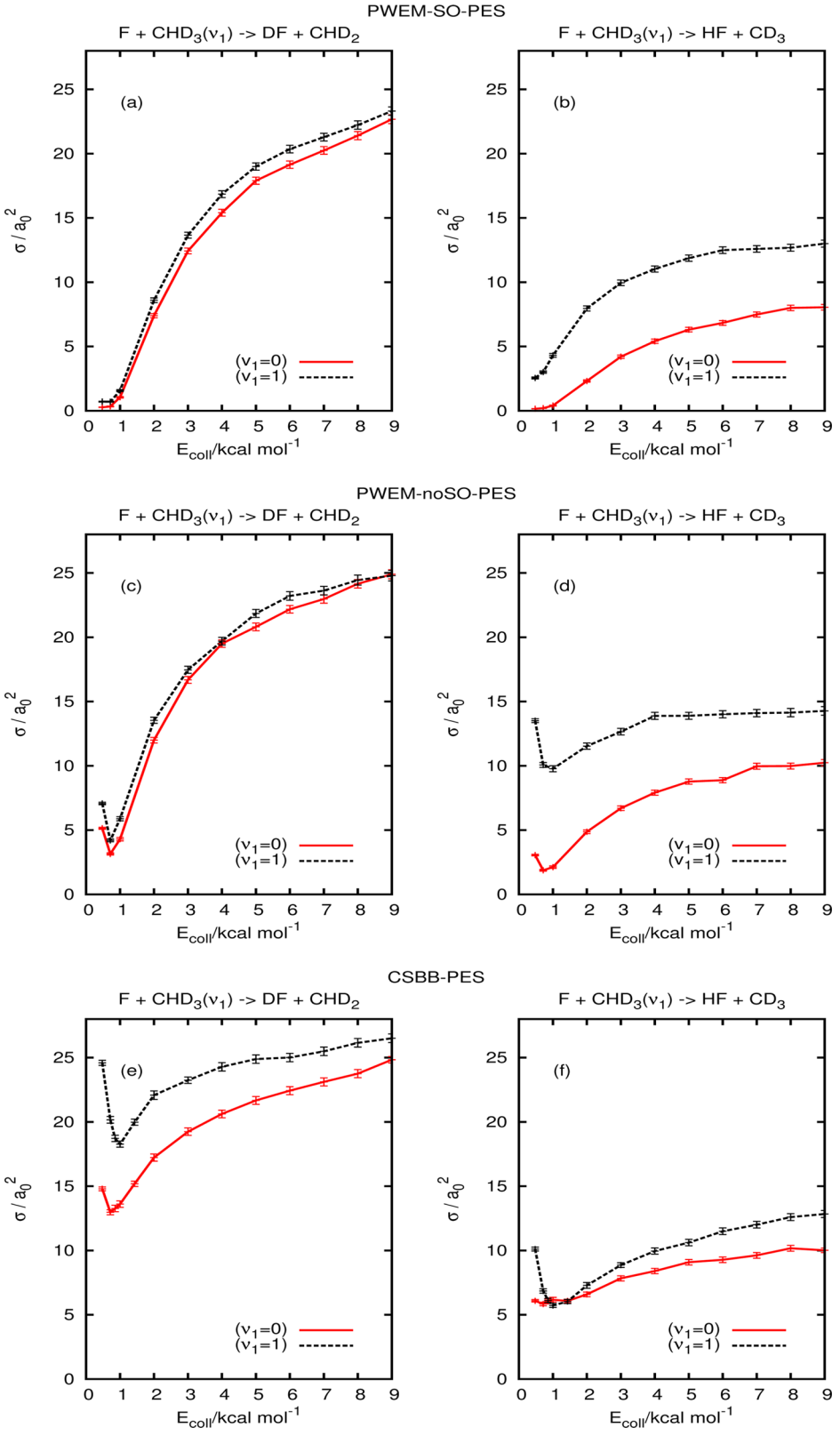

Figure 3. Excitation functions for the alternative product channels computed with different potential energy surfaces: (a, b) PWEM-SO-PES; (c, d) PWEM-noSO-PES; (e, f) CSBB-PES.

The QCT trajectories were ended when the C−F distance was larger than $22.0a_0$. Reactive trajectories were further analyzed to determine the partition of the total energy into relative and internal energies of the fragments. The rotational angular momenta of the product molecules were also determined. The final "quantum" states of HF or DF were assigned following the procedure outlined in ref 36. For completeness we briefly describe it here. First, the rotational

DOI: 10.1021/acs.jpca.5b06184
J. Phys. Chem. A XXXX, XXX, XXX−XXX

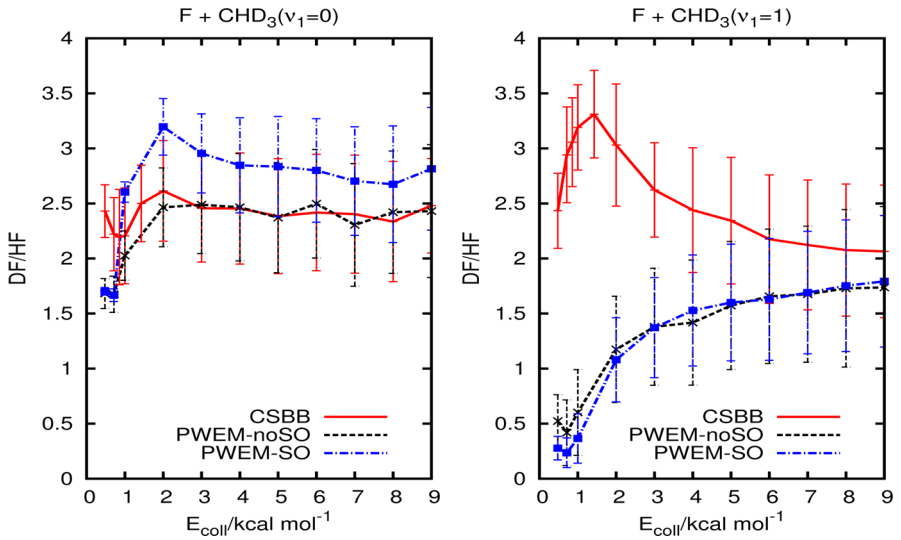

Figure 4. Effect of the C−H excitation on the branching ratios for the different surfaces.

quantum number of the diatomic fragment J was evaluated as the nearest integer satisfying $j = \sqrt{J(J+1)}$, where j is the classical angular momentum of the molecule in atomic units. The vibrational quantum number, ν, was then determined as the one that minimizes $|E_{int} - E_{\nu,J}|$, where E_{int} is the final internal energy of the fragment while $E_{\nu,J}$ is an eigenvalue of the rovibrational Hamiltonian of the diatomic molecule. The eigenvalues for HF and DF, with ν between 0 and 5 and J between 0 and 30, were numerically computed before running the trajectories, and they were given as an input to the QCT program. Good conservation of the total energy was checked by calculating the relative error $(E_{final} - E_{ini})/E_{ini}$ for each trajectory. The largest relative errors were found to be about 0.0003 with typical values being an order of magnitude smaller than that.

We have not applied any quantization scheme to the CD_3 and CHD_2 fragments because all these schemes enlarge the statistical uncertainty of the results. Previous experiences with the same reactive system have shown that alternative quantization criteria predict similar trends (i.e., the same qualitative behavior) even though they may afford quantitative differences.[23] In addition, all the schemes are arbitrary to some degree. This study mainly focuses on the disparate behavior predicted by three alternative PESs for the effect of the C−H excitation on the total reactivity. Because this effect can be analyzed without resorting to the quantization of the polyatomic products, which introduces the problems mentioned above, we chose the simplest and less uncertain option and avoided that quantization. Similarly, we do not discuss in detail QCT results computed by ignoring trajectories in which the products are formed with less internal energy than their zero point energy (ZPE restrained). The effect of this practice on QCT results has been discussed in ref 23 for the CSBB-PES and is similar for the other surfaces employed in this work. Just a short mention regarding ZPE-restrained results obtained with the PWEM-PESs is provided in the next section when it becomes pertinent.

Excitation functions were determined by running 30 000 trajectories per collisional energy (E_{coll}), for E_{coll} between 2.0 and 9.0 kcal/mol. At lower energies, we run 50 000 trajectories per energy. Extra sets of trajectories were run at 1.0 and 9.0 kcal/mol. Previous QCT calculations found that, at 1.0 kcal/mol, the vibrational excitation of the C−H bond produced the largest steering effect.[22,23] This was concluded after analyzing how the DF/HF branching ratio varied upon the excitation of CHD_3. Because the statistical uncertainty of the DF/HF ratio is about double that of the individual cross sections, while the value of the ratio itself is significantly smaller, the estimated relative uncertainty of the result is large. Therefore, at this energy, we run another set of 50 000 trajectories just to analyze the consistency of the observed DF/HF branching ratios. On the other hand, the recent experiments of Yang et al. evaluating the scattering angle distributions and the partitioning of the energy among the products were performed at 9.0 kcal/mol.[16] Determining these distributions from a QCT calculation requires us to distribute the reactive trajectories into different bins, corresponding to alternative values of the attribute under analysis. This procedure also increases the statistical uncertainty of the results. Therefore, at this energy, we run two different sets of 50 000 trajectories to evaluate the reproducibility of the resulting distributions.

RESULTS AND DISCUSSION

Effect of the C−H Excitation on Reactivity. Panels a and b of Figure 3 show the excitation functions predicted by the PWEM-SO surface, for the F + $CHD_3(\nu_1)$ → DF + CHD_2 and F + $CHD_3(\nu_1)$ → HF + CD_3 channels, respectively, with ν_1 = 0,1. To facilitate the comparison between alternative channels, the two pictures have been placed side by side, and the same range was used for the vertical axis. Figure 3c,d and 3e,f present the excitation functions computed with the PWEM-noSO and CSBB surfaces, respectively. According to the calculations performed on the PWEM-SO and PWEM-noSO surfaces, the excitation of the C−H bond has almost no effect on the cross sections for the DF + CHD_2 channel, but it significantly increases the yield of the HF + CD_3 channel. Therefore, the two PWEM surfaces predict an overall increase in reactivity upon the C−H excitation that mainly stems from the weakening of the C−H bond. This result contradicts the experiments of reported in refs 11 and 16. On the other hand, Figure 3e,f shows that the QCT results obtained with the CSBB surface also predict an overall increase in reactivity upon the C−H excitation. However, the curious finding in this case is that the yield of the DF + CHD_2 channel also increases with

DOI: 10.1021/acs.jpca.5b06184
J. Phys. Chem. A XXXX, XXX, XXX−XXX

the excitation of the C−H stretching vibration. Moreover, this increment is even larger than that of the HF + CD_3 channel, except at the higher energies where they become pretty similar.

It is observed that for both the CSBB-PES and PWEM-noSO-PES, the excitation functions present an unusual threshold behavior, with cross sections that increase while reducing the collisional energy beyond 1.0 kcal/mol. This effect was first described in ref 36, where it was shown that it is produced by an energy leak from the internal modes of methane to the translational motion (see Figure 10 of ref 22). Because of the pretty low barrier to reaction, even small energy leaks have an impact on the cross sections. As can be seen in Figure 3a,b and also in ref 37, a more typical behavior is recovered when running trajectories on surfaces that consider the SO effect, because they present a higher barrier to reaction.

It is also worth mentioning that, at very low energies, some trajectories form F-CHD_3 complexes that do not dissociate within the maximum time allowed by our trajectory setting (10.0 ps). This effect is significantly more notorious for the CSBB-PES. For example, at 1.0 kcal/mol and $\nu_1 = 0$, the cross section in atomic units for complex-forming trajectories is 0.68 ± 0.05 for the CSBB-PES, 0.09 ± 0.01 for the PWEM-noSO-PES, and 0.09 ± 0.01 for the PWEM-SO-PES. At 1.0 kcal/mol but for $\nu_1 = 1$, the corresponding cross sections are 0.77 ± 0.05 (CSBB-PES), 0.09 ± 0.01 (PWEM-noSO-PES), and 0.07 ± 0.01 (PWEM-SO-PES). This result can be explained by the pronounced wells present at the entrance channel of the CSBB-PES. The formation of these complexes favors the transfer of internal energy from CHD_3 to the relative motion of the reactive fragments and therefore promotes reaction at very low collisional energies.

It follows from the previous discussion that even though the PWEM surfaces and the CSBB surface predict an increase in the overall reactivity upon excitation of the C−H bond, the DF/HF branching ratios are going to be different. This discrepancy can be noted in Figure 4, which shows the results for the ground-state and the ν_1 excited-state reactions for the three surfaces. The PWEM-SO and the PWEM-noSO surfaces both predict that the excitation of the C−H stretch significantly reduces the DF/HF branching ratio. This ratio is not far from the statistical value for the ground-state reactant, except at very low energies. However, the DF/HF ratio falls below 2, in the whole energy range, when the C−H stretching is excited.

The CSBB surface, on the other hand, predicts a DF/HF ratio quite similar to that of the PWEM-noSO surface for the ground-state reaction. However, for the ν_1 excited-state reaction their outcomes differ, as the CSBB-PES predicts an increase in the DF/HF ratio instead of a decrease. This finding was first described in ref 22. Since then, it has been considered as giving support to the experimental results of Liu et al. The result has been rationalized by arguing that the C−H stretching excitation steers the F atom toward one of the C−D bonds (see ref 39 for a recent description). However, this effect is not observed in calculations performed with the PWEM surfaces. To confirm the discrepancy, extra sets of trajectories were run at E_{coll} = 1.0 kcal/mol, where the steering affect was found to be the largest. Thus, for a set of 100 000 trajectories, we found that the CSBB surface affords a DH/FH branching ratio of 3.27 ± 0.28 while the PWEM-noSO PES gives 0.61 ± 0.27, proving that the differences are significant and are larger than the statistical uncertainty of the results.

It has been discussed in ref 23 that, for the CSBB-PES, the application of ZPE constrains modifies the computed DF/HF branching ratio. In particular, it reduces the ratio for the ground-state reaction and increases it for the $\nu_1 = 1$ reaction. Similar trends were observed in this work for all the surfaces under analysis. We note, however, that this effect is relatively small and in no way modifies the fact that the DF/HF branching ratio diminishes upon the C−H excitation, when the reaction is studied with the PWEM surfaces. Thus, for example, at 1.0 kcal/mol the ZPE-constrained DF/HF branching ratio computed with the PWEM-SO PES is 1.94 ± 0.05 for the ground-state reaction and 0.46 ± 0.12 for the $\nu_1 = 1$ reaction. At 9.0 kcal/mol the corresponding figures are 2.52 ± 0.19 and 1.97 ± 0.23, respectively.

The computations presented in Figures 3 and 4 were obtained with the same program, using equivalent initial conditions. Therefore, the variations in the results can be traced only to differences in the PESs employed in each case. Not surprisingly, discrepancies are larger at very low energies where the trajectories are more sensitive to the details of the PES's topography. In Potential Energy Surfaces, we presented and discussed the differences between the three surfaces employed in this work. There we showed that the CSBB-PES has deeper and more extended wells in the entrance channel than the PWEM-PESs. Thus, altogether, the evidence collected in this work suggests that the strange steering effect observed in trajectories computed with the CSBB surface is caused by forces produced by the variety of relatively deep wells present at short C−F distances. However, as Figure 1 suggests, these features seem to be an artifact of the fitting.

Effect of the C−H Excitation on Product Distributions. Here we present various product distributions for the F + $CHD_3(\nu_1)$ → HF + CD_3 channel and compare them with the recent experimental findings of Yang et al.[16] For completeness we also show the results for the alternative product channel, even though the corresponding experimental distributions were not reported yet. The results presented in this section were obtained with the PWEM-SO surface, the most accurate surface among the ones employed in this work. The same collisional energy as in the experiment was used, and reactants in different vibrational states, $\nu_1 = 0$ and 1, were considered. Figure 5a presents the final vibrational state distribution of HF, and correspondingly, Figure 5b presents the final internal energy distribution of CD_3. These results perfectly agree with the experiments of Yang et al., who found that the extra energy put in the C−H bond is mostly channelled into the HF molecule while little effect is observed for CD_3. It is also noted that a significant fraction of the CD_3 molecules is formed with less energy than the ZPE. This fraction is larger for the ground-state reaction than for the excited-state reaction. Figure 5c presents the scattering angle distributions of CD_3, for both the ground-state and ν_1 excited-state reactions. In agreement with the experimental findings, it is observed that the two distributions are backward oriented and are pretty similar to each other. Figure 6a,b, showing the product energy distributions for the DF+CHD_2 channel, strongly contrast with Figure 5a,b. In this case, the distribution for the diatomic product is not affected by the excitation of the C−H bond, while the internal energy of the polyatomic product experiences a significant shift toward larger energies. Accordingly, the fraction of CHD_2 molecules formed with less energy than its ZPE is noticeable for the ground-state reaction but is significantly smaller for the ν_1 excited-state reaction. Altogether these pictures demonstrate that, at this high collisional energy, the fragment of CHD_3 that is not involved in the bond-breaking process mostly acts as a

DOI: 10.1021/acs.jpca.5b06184
J. Phys. Chem. A XXXX, XXX, XXX−XXX

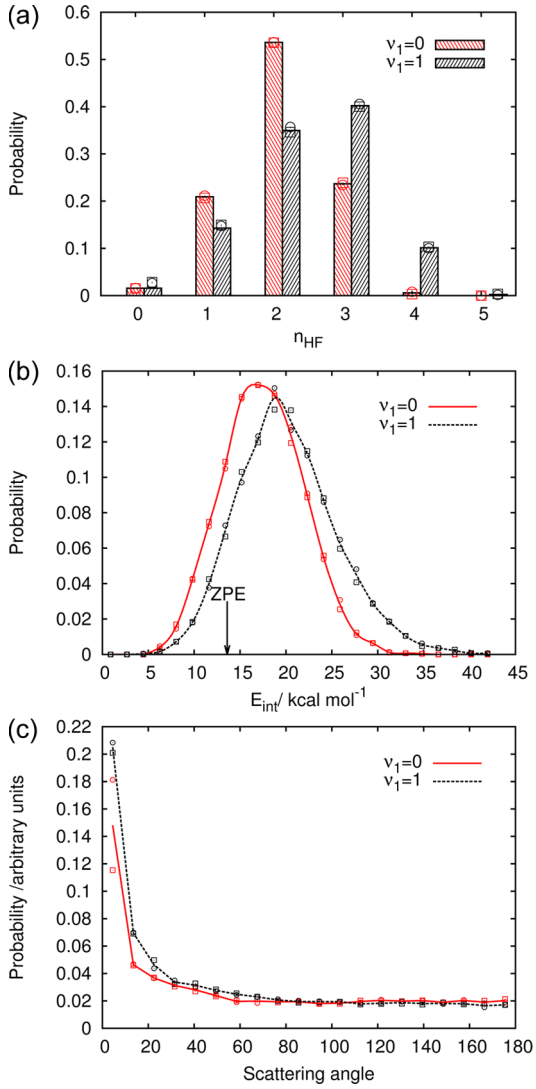

Figure 5. QCT results for F + $CHD_3(\nu_1 = 0, 1) \rightarrow HF + CD_3$ at E_{coll} = 9.0 kcal/mol. Circles and squares are used to plot the results of independent runs of 50 000 trajectories each. Lines correspond to results obtained considering the 100 000 trajectories altogether. (a) Vibrational state distribution for HF; (b) internal energy distribution for CD_3 with arrow indicating the ZPE of the fragment; (c) scattering angle distribution for CD_3 in the center-of-mass frame.

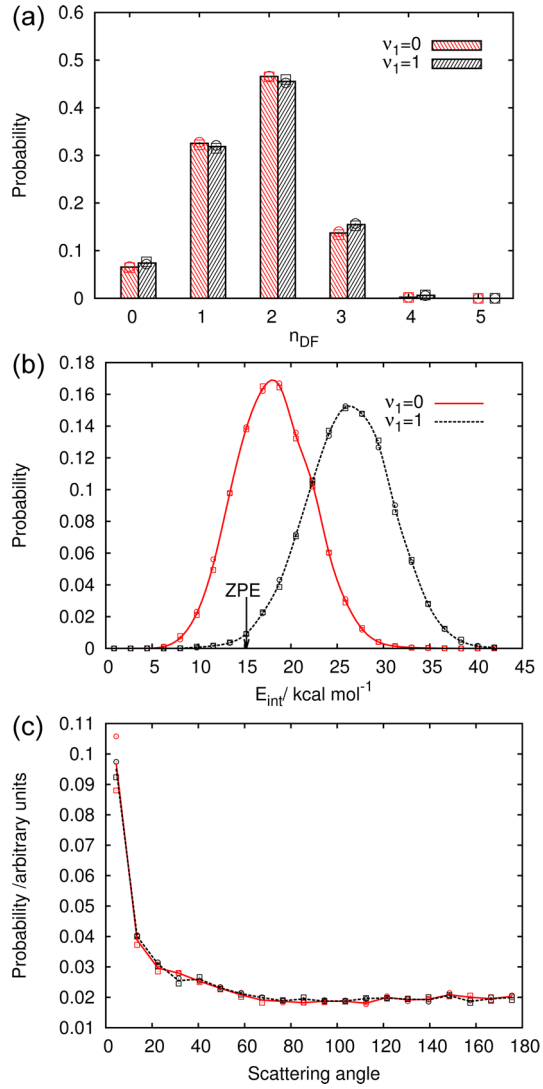

Figure 6. QCT results for F + $CHD_3(\nu_1 = 0, 1) \rightarrow DF + CHD_2$ at E_{coll} = 9.0 kcal/mol. Circles and squares are used to plot the results of independent runs of 50 000 trajectories each. Lines correspond to results obtained considering the 100 000 trajectories altogether. (a) Vibrational state distribution for DF; (b) internal energy distribution for CHD_2 with the arrow indicating the ZPE of the fragment; (c) scattering angle distribution for CHD_2 in the center-of-mass frame.

spectator, maintaining its internal energy in going from reactants to products. On the contrary, the energy located in the bond being broken is strongly involved in the reactive event, and its energy is channelled into the diatomic product. Finally, the comparison between Figures 5c and 6c shows that, for both channels, the polyatomic products are scattered in the backward direction.

It has to be mentioned that, when the distributions shown in Figure 5 and 6 are computed with the CSBB-PES, the results are rather similar. This is not surprising because the product energy distributions are mainly dictated by the topography of the PES on the product channel and both CSBB-PES and PWEM-SO-PES are exactly the same in that region. The scattering angle distributions, on the other hand, could be influenced by the shape and depth of the wells at the entrance channel. However, this influence is expected to decrease with the collisional energy and should be negligible at the very high energies evaluated in the experiment.

CONCLUSIONS

We have performed QCT calculations aimed at elucidating the effect of exciting the C−H bond in F + CHD_3 collisions, employing three alternative potential energy surfaces: the CSBB-PES, the PWEM-noSO-PES, and the PWEM-SO-PES. The results obtained with the different surfaces were thoroughly compared with each other and with recent experiments of Zhang et al.[11] and Yang et al.[16] Product distributions were also computed and analyzed.

Results computed with the PWEM surfaces disagree with those of the CSBB-PES in regard to the effect of exciting the C−H bond. The PWEM surfaces indicate that the excited C−H bond is significantly more reactive than the ground-state one, while the reactivity of the C−D bonds is almost the same. The CSBB-PES, on the other hand, predicts that the reactivity of the C−D bonds increases even more than that of the C−H bond. Therefore, the DF/HF branching ratios afforded by the

DOI: 10.1021/acs.jpca.5b06184
J. Phys. Chem. A XXXX, XXX, XXX−XXX

PWEM-SO-PESs, and the CSBB-PES differ. On the other hand, all the surfaces agree at indicating that the overall reactivity increases with the excitation of the C−H bond, in the whole energy range. This prediction contradicts the experimental results Zhang et al.[11] and Yang et al.,[16] who reported a deleterious effect at low and high collisional energies, respectively. Finally, product energy and scattering angle distributions are pretty similar for all the surfaces. This is not surprising because the product channel is the same in the three PESs. In this case, QCT results agree with the experimental findings.

Differences between experimental findings and theoretical predictions can be ascribed to different sources. From the theoretical side, errors can originate from limitations of the PES or from approximations introduced in the dynamical computations. For the calculations presented here, mainly for those computed with the PWEM-SO-PES, the weakest part seems to be in the dynamics. On one side, we used classical mechanics to describe the movements of the nuclei. Thus, our computations lack important quantum mechanical ingredients like the restrictions imposed on the dynamics by the ZPE of the modes perpendicular to the reaction coordinate. Nevertheless, it is difficult to believe that these shortcomings could be the cause of the discrepancies found between QCT calculations and experimental results. On the other hand, we assumed that the reaction occurs on a single potential energy surface while there are, in fact, three low-lying coupled surfaces and only one of them connects reactants to products. If the probability of nonadiabatic transitions is altered by the excitation of the C−H stretching, the reactivity of CHD_3 could also be altered. We close this article by noting that previous disagreements between theory and experiments have been the driving force in the pursuit of better experiments and more accurate calculations. This eventually led to a better understanding of the reactions under consideration. We hope that the results presented here are just another sample of this trend.

AUTHOR INFORMATION

Corresponding Authors

*E-mail: juliana@unq.edu.ar.

*E-mail: uwe.manthe@uni-bielefeld.de.

Notes

The authors declare no competing financial interest.

ACKNOWLEDGMENTS

The authors thank Till Westermann for many discussions and suggestions regarding the PESs and Gabor Czakó and Joel Bowman for sharing their surface with us. Financial support by the Deutsche Forschungsgemeinschaft is gratefully acknowledged. J.P. is very grateful to the Universidad de Quilmes, ANCyT, and CONICET for financial support.

REFERENCES

(1) Lin, J.; Zhou, J.; Shiu, W.; Liu, K. State-specific correlation of coincident product pairs in the F + CD_4 reaction. *Science* **2003**, *300*, 966−969.

(2) Zhou, J.; Lin, J.; Shiu, W.; Pu, S.-C.; Liu, K. Crossed-beam scattering of F+CD_4→DF+CD_3(νNK): The integral cross sections. *J. Chem. Phys.* **2003**, *119*, 2538−2544.

(3) Zhou, J.; Lin, J.; Shiu, W.; Liu, K. Insights into dynamics of the F +CD_4 reaction via product pair correlation. *J. Chem. Phys.* **2003**, *119*, 4997−5000.

(4) Zhou, J.; Lin, J.; Liu, K. Mode-correlated product pairs in the F +CHD_3→DF+CHD_2 reaction. *J. Chem. Phys.* **2003**, *119*, 8289−8296.

(5) Zhou, J.; Shiu, W.; Lin, J.; Liu, K. Rotationally selected product pair correlation in F+CD_4→DF(ν')+CD_3(ν = 0.N). *J. Chem. Phys.* **2004**, *120*, 5863−5866.

(6) Shiu, W.; Lin, J.; Liu, K. Reactive resonance in a polyatomic reaction. *Phys. Rev. Lett.* **2004**, *92*, 103201.

(7) Zhou, J.; Lin, J.; Liu, K. Observation of a reactive resonance in the integral cross section of a six-atom reaction: F+CHD_3. *J. Chem. Phys.* **2004**, *121*, 813−818.

(8) Zhou, J.; Shiu, W.; Lin, J.; Liu, K. Rotationally selected product pair correlation: F+CD_4→DF(ν')+CD_3(ν_2 = 0 and 2,N). *J. Chem. Phys.* **2006**, *124*, 104309.

(9) Zhou, J.; Lin, J.; Shiu, W.; Liu, K. State-correlation matrix of the product pair from F + CD_4 → DF(ν') + CD_3(0,ν_2,0,0). *Phys. Chem. Chem. Phys.* **2006**, *8*, 3000−3006.

(10) Zhang, B.; Yan, S.; Liu, K. Unraveling multicomponent images by extended cross correlation analysis. *J. Phys. Chem. A* **2007**, *111*, 9263−2968.

(11) Zhang, W.; Kawamata, H.; Liu, K. C-H Stretching excitation in the early barrier F + CHD_3 reaction inhibits C-H bond cleavage. *Science* **2009**, *325*, 303−306.

(12) Czakó, G.; Shuai, Q.; Liu, K.; Bowman, J. M. Communication: Experimental and theoretical investigations of the effects of the reactant bending excitations in the F+CHD_3 reaction. *J. Chem. Phys.* **2010**, *133*, 131101.

(13) Harper, W. W.; Nizkorodov, S. A.; Nesbitt, D. J. Quantum state-resolved reactive scattering of F+CH_4→HF(v_iJ)+CH_3: Nascent HF(v_iJ) product state distributions. *J. Chem. Phys.* **2000**, *113*, 3670−3680.

(14) Shiu, W.; Lin, J. J.; Liu, K.; Wu, M.; Parker, D. H. Imaging the pair-correlated excitation function: The F+CH_4→HF(ν')+CH_3(ν = 0) reaction. *J. Chem. Phys.* **2004**, *120*, 117−122.

(15) Kawamata, H.; Zhang, W.; Liu, K. Imaging the effects of the antisymmetric stretch excitation of CH_4 in the reaction with F atoms. *Faraday Discuss.* **2012**, *157*, 89−100.

(16) Yang, J.; Zhang, D.; Jiang, B.; Dai, D.; Wu, G.; Zhang, D.; Yang, X. How Is CH Vibrational Energy Redistributed in F + CHD_3(ν_1 = 1) → HF + CD_3 ? *J. Phys. Chem. Lett.* **2014**, *5*, 1790−1794.

(17) Yacovitch, T. I.; Garand, E.; Kim, J. B.; Hock, C.; Theis, T.; Neumark, D. M. Vibrationally resolved transition state spectroscopy of the F+H_2 and F+CH_4 reactions. *Faraday Discuss.* **2012**, *157*, 399−414.

(18) Cheng, M.; Feng, Y.; Du, Y.; Zhu, Q.; Zheng, W.; Czakó, G.; Bowman, J. M. Communication: Probing the entrance channels of the X + CH_4→HX + CH_3 (X = F, Cl, Br, I) reactions via photodetachment of $XCH_4(-)$]. *J. Chem. Phys.* **2011**, *134*, 191102.

(19) Palma, J.; Manthe, U. A full-dimensional wave packet dynamics study of the photodetachment spectra of $FCH_4(-)$. *J. Chem. Phys.* **2012**, *137*, 044306.

(20) Westermann, T.; Eisfeld, W.; Manthe, U. Coupled potential energy surface for the F(^{2}P) + CH_4 → HF + CH_3 entrance channel and quantum dynamics of the CH_4F photodetachment. *J. Chem. Phys.* **2013**, *139*, 014309.

(21) Westermann, T.; Kim, J. B.; Weichman, M. L.; Hock, C.; Yacovitch, T. I.; Palma, J.; Neumark, D. M.; Manthe, U. Resonances in the entrance channel of the elementary chemical reaction of fluorine and methane. *Angew. Chem., Int. Ed.* **2014**, *53*, 1122−1126.

(22) Czakó, G.; Bowman, J. M. C-H stretching excitation steers the F atom to the C-D bond in the F + CHD_3 reaction. *J. Am. Chem. Soc.* **2009**, *131*, 17534−17535.

(23) Czakó, G.; Bowman, J. M. Quasiclassical trajectory calculations of correlated product distributions for the F+CHD_3(ν_1 = 0,1) reactions using an ab initio potential energy surface. *J. Chem. Phys.* **2009**, *131*, 244302.

(24) Tian, X.; Gao, T.; He, N.; Zhang, Z. Direct ab initio molecular dynamics study of F atom reaction with methane. *Mol. Phys.* **2008**, *106*, 2717−2724.

DOI: 10.1021/acs.jpca.5b06184
J. Phys. Chem. A XXXX, XXX, XXX−XXX

(25) Espinosa-García, J. Quasiclassical trajectory calculations analyzing the role of vibrational and translational energy in the F +CH_2D_2 reaction. *J. Chem. Phys.* **2009**, *130*, 054305.
(26) Espinosa-García, J.; Bravo, J. L. State-to-State dynamics analysis of the F + CHD_3 reaction: a quasiclassical trajectory study. *J. Phys. Chem. A* **2008**, *112*, 6059−6065.
(27) Espinosa-García, J. Quasi-classical trajectory study of the F + CD_4 reaction dynamics. *J. Phys. Chem. A* **2007**, *111*, 3497−3501.
(28) Espinosa-García, J. Vibrational versus translational energies in the F + CH_4 reaction: A comparison with the F + CH_2D_2 reaction using quasi-classical trajectory methods. *Chem. Phys. Lett.* **2010**, *488*, 153−157.
(29) Troya, D.; Millán, J.; Baños, I.; González, M. Ab initio potential energy surface, variational transition state theory, and quasiclassical trajectory studies of the F+CH_4→HF+CH_3 reaction. *J. Chem. Phys.* **2004**, *120*, 5181−5191.
(30) Castillo, J. F.; Aoiz, F. J.; Bañares, L.; Martinez-Nuñez, E.; Fernández-Ramos, A.; Vazquez, S. Quasiclassical trajectory study of the F + CH_4 reaction dynamics on a dual-level interpolated potential energy surface. *J. Phys. Chem. A* **2005**, *109*, 8459−8470.
(31) Troya, D. Ab initio and direct quasiclassical-trajectory study of the F+CH_4→HF+CH_3 reaction. *J. Chem. Phys.* **2005**, *123*, 214305.
(32) Layfield, J. P.; Sweeney, A. F.; Troya, D. Direct-dynamics study of the F + CH_4, C_2H_6, C_3H_8, and i-C_4H_{10} reactions. *J. Phys. Chem. A* **2009**, *113*, 4294−4304.
(33) Chu, T.; Han, K.; Espinosa-García, J. A five-dimensional quantum dynamics study of the F(^{2}P)+CH_4 reaction. *J. Chem. Phys.* **2009**, *131*, 244303.
(34) Nyman, G.; Espinosa-García, J. Reduced dimensionality quantum scattering calculations on the F + CH_4 → FH + CH_3 reaction. *J. Phys. Chem. A* **2007**, *111*, 11943−11947.
(35) Wang, D.; Czakó, G. Quantum Dynamics Study of the F + CH_4 → HF + CH_3 Reaction on an Ab Initio Potential Energy Surface. *J. Phys. Chem. A* **2013**, *117*, 7124−7130.
(36) Czakó, G.; Shepler, B. C.; Braams, B. J.; Bowman, J. M. Accurate ab initio potential energy surface, dynamics, and thermochemistry of the F+CH_4→HF+CH_3 reaction. *J. Chem. Phys.* **2009**, *130*, 084301.
(37) Czakó, G.; Bowman, J. M. An ab initio spin-orbit-corrected potential energy surface and dynamics for the F + CH_4 and F + CHD_3 reactions. *Phys. Chem. Chem. Phys.* **2011**, *13*, 8306−8312.
(38) Raff, L.; Thompson, D. The classical trajectory approach to reactive scattering. In *Theory of Chemical Reaction Dynamics*; Baer, M., Ed.; CRC Press: Boca Raton, FL, 1985; Chapter 1.
(39) Liu, K. Perspective: Vibrational-induced steric effects in bimolecular reactions. *J. Chem. Phys.* **2015**, *142*, 080901.

DOI: 10.1021/acs.jpca.5b06184
J. Phys. Chem. A XXXX, XXX, XXX−XXX